Journal of Quantitative Spectroscopy & Radiative Transfer 144 (2014) 11–26

Contents lists available at ScienceDirect

Journal of Quantitative Spectroscopy & Radiative Transfer

journal homepage: www.elsevier.com/locate/jqsrt

High resolution study of $^{M}GeH_4$ ($M=76$, 74) in the dyad region

O.N. Ulenikov [a,b,*], O.V. Gromova [a,b], E.S. Bekhtereva [a,b], N.I. Raspopova [a,b], P.G. Sennikov [c], M.A. Koshelev [c,d,e], I.A. Velmuzhova [c], A.P. Velmuzhov [c,e], A.D. Bulanov [c,e]

[a] Institute of Physics and Technology, National Research Tomsk Polytechnic University, Tomsk 634050, Russia
[b] Physics Department, National Research Tomsk State University, Tomsk 634050, Russia
[c] G.G. Devyatykh Institute of Chemistry of High Purity Substances, Russian Academy of Sciences, 603950 Nizhny Novgorod, Russia
[d] Institute of Applied Physics, Russian Academy of Sciences, 603950 Nizhny Novgorod, Russia
[e] N.I. Lobachevsky State University of Nizhni Novgorod, National Research University, 603950 Nizhny Novgorod, Russia

ARTICLE INFO

Article history:
Received 17 November 2013
Received in revised form
20 March 2014
Accepted 23 March 2014
Available online 29 March 2014

Keywords:
Dyad of GeH_4 states
High resolution spectra of GeH_4
Spectroscopic parameters

ABSTRACT

The infrared spectrum of GeH_4 (88.1% of $^{76}GeH_4$, 11.5% of $^{74}GeH_4$, and minor amounts of three other stable isotopic species in the sample) was measured in the 700–1080 cm^{-1} region with a Bruker IFS 125HR Fourier transform interferometer (Nizhny Novgorod, Russia) and analyzed. 1922 transitions with $J^{max.}=26$ were assigned to the ν_4 and ν_2 bands of $^{76}GeH_4$ (ν_2 is a symmetry forbidden absorption band, and its transitions appear in the spectrum only because of strong Coriolis interaction with the ν_4 band). Rotational, centrifugal distortion, tetrahedral splitting, and interaction parameters for the ground, (0100) and (0001) vibrational states were determined from the fit of experimental line positions. The obtained set of parameters reproduces the initial experimental data with an accuracy close to experimental uncertainties. The result of analogous analysis of the $^{74}GeH_4$ isotopologue (the number of assigned transitions is 788) is also presented.

1. Introduction

Germane in a natural isotopic composition is used for producing high-purity germanium. Various physical devices (*e.g.*, high-sensitivity detectors of nuclear radiation) are manufactured on its base [1]. Germane is one of the important components of the atmospheres of giant gas-planets, such as Jupiter and Saturn [2–4], and its presence should be taken into account when studying their atmospheric composition and chemistry. In particular, in the atmospheres of Jupiter and Saturn germane was detected at abundances orders of magnitude greater than their thermochemical equilibrium values in the upper tropospheres [5]. For that reason, laboratory investigations of high resolution spectra of germane are interesting and important.

Germane in a natural isotopic composition produces complex infrared spectra, first of all because of the existence of five stable isotopologues with mass numbers 70 (20.55%), 72 (27.37%), 73 (7.67%), 74 (36.74%), and 76 (7.67%). Additional complexity of the germane spectra arises from the presence of very strong Coriolis interaction between its two deformational fundamentals ν_2 and ν_4. GeH_4 is a spherical top molecule, hence, it has no permanent dipole moment, and capabilities of the Ground State Combination Differences method (which is very efficient for studying the molecules of other type) are very limited as applied to germane.

Spectra of different $^{M}GeH_4$ ($M=70$, 72, 73, 74, 76) isotopologues of germane were the objects of study for

* Corresponding author. Institute of Physics and Technology, National Research Tomsk Polytechnic University, Tomsk 634050, Russia.
E-mail address: Ulenikov@mail.ru (O.N. Ulenikov).

http://dx.doi.org/10.1016/j.jqsrt.2014.03.025
0022-4073/

many years (see, *e.g.*, Refs. [6–40]). Up to 1972 the spectra were recorded with low or medium resolution. Starting with 1973, Oka with co-authors extensively studied pure rotational spectra of the XH_4 (T_d symmetry) molecules (X=C, Ge, Si) by the method of infrared-microwave double resonance [17–21]. The first high resolution infrared spectrum of germane (ν_3 and $2\nu_3$ bands of all five isotopologues) was studied in Ref.[25]. High resolution spectra of high excited overtone stretching bands of germane were extensively discussed in a number of papers by Zhu and co-authors [34–40], in the frame of the local mode model. As to the bending bands, only the ν_2 and ν_4 fundamentals were analyzed earlier with high resolution [27,29,31,32]. Besides, only spectra in separate narrow regions of the ν_2 and ν_4 bands were discussed even for the mostly abundant germane species. For that reason, high resolution analysis of the ν_2 and ν_4 bands of any isotopic species of germane in a wide spectral region is suitable and timely.

In this paper we present results of the analysis of the high resolution Fourier transformed spectrum of $^{M}GeH_4$ (M=74, 76) in the 700–1080 cm^{-1} region where the ν_2 and ν_4 bands are located. The experimental details are given in Section 2. The theoretical background of our study is briefly discussed in Section 3. Results and discussion are presented in Section 4.

2. Experimental details

A sample of germane containing $^{76}GeH_4$ (88.1%), $^{74}GeH_4$ (11.5%), $^{73}GeH_4$ (0.07%), $^{72}GeH_4$ (0.17%), and $^{70}GeH_4$ (0.12%) was used in the present study. First, the sample of germane in natural abundance was synthesized at the Institute of Chemistry of High-Purity Substances of the Russian Academy of Sciences by a reaction between $GeCl_4$ and sodium borohydride with subsequent purification by the rectification method. Then the sample was enriched with the ^{76}Ge isotope using the centrifugal method at the Joint Stock Company "Production Association Electrochemical Plant", Zelenogorsk, Russia. The enriched sample was repeatedly purified by the rectification method. Finally, the amount of hydrocarbon, carbon dioxide, di-, and tri-germane impurities in the sample enriched with ^{76}Ge was less than 10^{-5} mol%, 10^{-4} mol%, 10^{-1}–10^{-3} mol %, respectively. The amount of the other impurities was less than 3×10^{-5} mol%

The high-resolution spectra of GeH_4 were recorded at room temperature in the 700–1080 cm^{-1} wavenumber range with a Bruker IFS125HR Fourier transform spectrometer (Institute of Chemistry of High-Purity Substances, Nizhny Novgorod, Russia) equipped with a Globar source, a KBr beamsplitter and a liquid nitrogen cooled mercury–cadmium–telluride detector. The aperture size was 1.7 mm. The resolution due to the maximum optical path difference was 0.003 cm^{-1} and the Norton-Beer (weak) apodization function was applied. A single-pass 20-cm cell equipped with ZnSe windows was permanently connected to the vacuum system with a gas sample vacuum system, a turbo-molecular pump, and pressure gauges covering the 10^{-3}–100 Torr pressure range. The optical compartment of the spectrometer was evacuated by a mechanical pump down to 0.02 Torr and remained at that pressure during the experiment.

Experimental spectra (see Fig. 1) were obtained by averaging 1000 scans. The spectra were recorded at significantly different pressures, 0.4 (spectrum W) and 10 (spectrum S) Torr, to cover a wider range of J numbers and to estimate the value of possible systematic errors in the line positions caused by pressure shifts. Comparison of the positions of unsaturated unblended lines in two spectra recorded at a pressure of 0.4 and 10 Torr shows a good agreement between the pairs of lines within $\pm$ 10^{-5} cm^{-1}, which demonstrates a negligible effect of the pressure shift. The spectra were calibrated with 400 OCS peaks of the ν_1 and $2\nu_2$ bands (centered at 860 cm^{-1} and 1047 cm^{-1}, respectively), and NIST calibration tables [41], based on heterodyne frequency measurements. After calibration the standard deviation of the difference between the measured and tabulated peak positions was less than 10^{-4} cm^{-1}.

3. Irreducible tensorial sets and effective Hamiltonian of the XY_4 (T_d) molecule

Germane is a spherical top molecule of the T_d symmetry. This molecule has a tetrahedral structure resulting in one nondegenerate (q_1, A_1), one doubly degenerate (q_2, E), and two triply degenerate (q_3 and q_4, F_2) vibrational modes. In this case, the ν_2 and ν_4 fundamentals are connected by a very strong Coriolis interaction. As a consequence, the spectrum of the ν_2 and ν_4 bands may be described only in the frame of the effective Hamiltonian model which takes into account the interaction between the $(0100, E)$ and $(0001, F_2)$ states. On the other hand, high symmetry of the molecule necessitates using a special mathematical formalism (the theory of Irreducible Tensorial Sets, see, *e.g.*, Refs. [45–48] and recent review in Ref. [54]) for description of its spectra. Application of the mentioned formalism to the XY_4 (T_d) molecules was discussed in the spectroscopic literature many times (see, *e.g.*, Refs. [42–44]). For that reason we present here very briefly only the main points necessary for understanding the structure of the Fortran code discussed in Section 3.

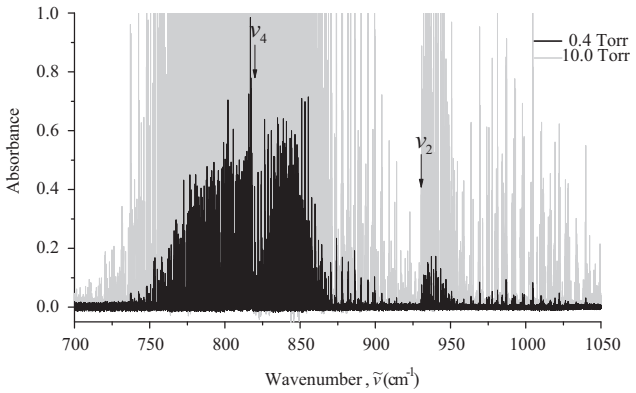

Fig. 1. Survey spectrum of $^{76}GeH_4$ and $^{74}GeH_4$ in the region of the dyad. Experimental conditions: absorption path length is 20 cm; room temperature; number of scans is 1000; sample pressure is 0.4 Torr for the "black" spectrum and 10 Torr for the "grey" spectrum.

3.1. Irreducible rotational operators

(a) *Irreducible rotational operators of the SO(3) group*: In accordance with general statements of the Irreducible Tensorial Sets Theory [45–47], the basic first-rank irreducible rotational operators $R_m^{\Omega(K)}$ ($m=0, \pm 1, \ldots, \pm K$) can be chosen in the following form:

$$R_1^{1(1)} = -\frac{1}{\sqrt{2}}\left(J_x - iJ_y\right) \equiv -J_+,$$
$$R_{-1}^{1(1)} = \frac{1}{\sqrt{2}}\left(J_x + iJ_y\right) \equiv J_-,$$
$$R_0^{1(1)} = J_z \equiv J_0. \quad (1)$$

In the operators $R_m^{\Omega(K)}$ the following notation is used: Ω is the total degree of rotational operators J_α, α=x, y, z (for example, for $\Omega=1$, $R_{\ldots}^{1(\ldots)} \sim J_\alpha$; for $\Omega=2$, $R_{\ldots}^{2(\ldots)} \sim J_\alpha J_\beta$; *etc.*); the indices K and m indicate the irreducible representation $D^{(K)}$ of the $SO(3)$ symmetry group and its line; the operators J_α are conventional angular momentum components related to the molecular fixed coordinate system:

$$J_x = i\frac{\cos\varphi}{\sin\theta}\left(\frac{\partial}{\partial\psi} - \cos\theta\frac{\partial}{\partial\varphi}\right) - i\sin\varphi\frac{\partial}{\partial\theta},$$
$$J_y = -i\frac{\sin\varphi}{\sin\theta}\left(\frac{\partial}{\partial\psi} - \cos\theta\frac{\partial}{\partial\varphi}\right) - i\cos\varphi\frac{\partial}{\partial\theta}, \quad (2)$$

and

$$J_z = -i\frac{\partial}{\partial\varphi}. \quad (3)$$

The irreducible rotational operators $R_{\tilde m}^{\Omega+1(K+1)}$ may be constructed from the corresponding irreducible rotational operators $R_m^{\Omega(K)}$ ($n=0, \pm 1, \ldots \pm K$) and $R_l^{1(1)}$ ($l=0, \pm 1$) of lower degrees and ranks in accordance with the general rule [49,50],

$$R_{\tilde m}^{\Omega+1(K+1)} = \sum_{l=-1,0,1} C_{K\ \tilde m-l,1\ l}^{K+1\ \tilde m} R_{\tilde m-l}^{\Omega(K)} R_l^{1(1)}, \quad (4)$$

where $C_{K\ \tilde m-l,1\ l}^{K+1\ \tilde m}$ are known Clebsh–Gordan coefficients, Ref. [47]. The irreducible rotational operators $R_m^{\Omega(K)}$ with $K<\Omega$ (in this case, the parity of both Ω and K must be the same [49]) are constructed as

$$R_m^{\Omega(K)} = R_m^{\Omega=K(K)}(R^{2(0)})^{(\Omega-K)/2}, \quad (5)$$

where we use the notation $R^{2(0)} = (J_x^2 + J_y^2 + J_z^2)$. As an illustration, Appendix A presents the operators $R_m^{\Omega(K)}$ for $\Omega \le 3$.

(b) *Irreducible rotational operators of the* T_d *group*: Different rotational operators $R_\sigma^{\Omega(K,n\Gamma)}$, that are symmetrized in accordance with irreducible representations $\Gamma = A_1$, A_2, E, F_1, or F_2 of the T_d symmetry group, can be easily constructed from the above discussed operators $R_m^{\Omega(K)}$ by using the following general relations [49]:

$$R_\sigma^{\Omega(K,n\Gamma)} = \sum_m {}^{(K)}G_{n\Gamma\sigma}^m R_m^{\Omega(K)}. \quad (6)$$

The reduction matrix elements ${}^{(K)}G_{n\Gamma\sigma}^m$, which are presented in Eq. (6), are determined by a concrete point symmetry group. Speaking about molecules of the T_d symmetry, only numerical representation of the ${}^{(K)}G_{n\Gamma\sigma}^m$ values was used (see, *e.g.*, Refs. [43,51,52]). In our case, we used a much more convenient analytical representation of G-matrix elements. For convenience of the reader, they are reproduced from Refs. [53,54] in Appendix B. We do not discuss here why the index n is defined in the formulas of Appendix B in such a form. This issue was discussed in detail in the original papers [53,54], and we think that the reproduction of all arguments in the present paper is excessive. We will mention only that the definition of the index n for the ${}^{(J)}G_{n\Gamma\sigma}^m$ matrix elements in the formulas of Appendix B differs from the definition used, *e.g.*, in Refs. [43,51,52]. In the mentioned works the index n takes on the values 1, 2, 3,…, and the increase of the value n follows the increase of the energy values of states of the same symmetry. In our case, the value of n is defined exclusively by the value of the corresponding index in the right hand sides of Eqs. (14)–(18). At the same time, we would like to note that there is no contradiction between these two definitions of G-matrix elements. One should remember that the main reason for introducing the index n is to distinguish between different wave functions (or operators) of the same symmetry. From this point of view both definitions of n are equivalent. Moreover, for small values of quantum number J both definitions of G-matrix elements coincide completely. For large values of quantum number J there may appear a difference between the values of G-matrix elements. However, it does not contradict the general theory of symmetry because even different definitions of G-matrices are nothing but different reductions of irreducible representations of the $SO(3)$ group to irreducible representations of the T_d symmetry group. As a consequence, it should not influence the final result.

We would like to make here one more minor remark. In spite of the fact that the analytical presentation of G-matrix elements with n-index definition from Appendix B (as a consequence, analytical presentation of numerous intermediate results) is considerably more suitable than a numerical one, namely the n-index definition from [43,51,52] is most convenient and simple for a final description of ro-vibrational energy levels and transitions. For that reason, the analysis and all calculations in the present paper have been made with the G-matrix defined in Appendix B, but the notation of indices n/n' in the final results (Tables 2 and 8, and Supplementary materials) follows Refs. [43,51,52], *i.e.*, indices n and n' take on the values 1, 2, 3,…, and for any vibrational state increase with increasing energy values of states of the same symmetry.

3.2. Ro-vibrational functions in the symmetrized form

As the T_d symmetry group has five irreducible representations A_1, A_2, E (E_1 or E_2), F_1 (F_{1x}, F_{1y}, F_{1z}) and F_2 (F_{2x}, F_{2y}, F_{2z}), any vibrational–rotational wave function should be totally symmetric (A_1), antisymmetric (A_2), or be transformed under symmetry operations according to one of the two (E_1 or E_2), or three (F_{1x}, F_{1y}, F_{1z}), (F_{2x}, F_{2y}, F_{2z}) lines of the irreducible representations E, F_1, F_2. In a general case, any vibrational–rotational function can be constructed in the following form [49,55]:

$$|v\gamma_v; Jn_J\gamma_r; m\gamma s\rangle \equiv (|v\gamma_v\rangle \otimes |Jn_J\gamma_r\rangle)_s^\gamma = \sqrt{[\gamma]}\sum_{\sigma_v\sigma_r}\begin{pmatrix}\gamma & \gamma_v & \gamma_r\\ s & \sigma_v & \sigma_r\end{pmatrix}|v\gamma_v\sigma_v\rangle|Jn_J\gamma_r\sigma_r\rangle, \quad (7)$$

where the set of indices $v\gamma_v$, $Jn_J\gamma_r$, and $m\gamma s$ unambiguously determines any vibrational–rotational function symmetrized

in the T_d group, and the indices γ_v, γ_r, and γ are the symmetry of vibrational, rotational, and vibrational–rotational functions, respectively. The $|v\gamma_v\sigma_v\rangle$ and $|Jn_J\gamma_r\sigma_r\rangle$ in Eq. (7) are pure vibrational and rotational wave functions symmetrized in the T_d group; the symbols $\otimes$ and $[\gamma]$ denote direct tensorial product and dimension of the irreducible representation γ, respectively; the values

$$\begin{pmatrix} \gamma & \gamma_v & \gamma_r \\ s & \sigma_v & \sigma_r \end{pmatrix}$$

are the so-called 3Γ-symbols of the T_d symmetry group (nonzero 3Γ-symbols are presented in Appendix C).

The pure rotational functions, $|Jn_J\gamma_r\sigma_r\rangle$, being the functions symmetrized in the T_d symmetry group, can be constructed in accordance with the general equation analogous to Eq. (6):

$$|Jn_J\gamma_r\sigma_r\rangle = \sum_k {}^{(J)}G^k_{n_J\gamma_r\sigma_r}|Jk\rangle. \tag{8}$$

Here the coefficients ${}^{(J)}G^k_{n_J\gamma_r\sigma_r}$ can be determined in accordance with formulas of Appendix B; the $|Jk\rangle$ $(-J \le k \le J)$ are the conventional rotational functions for which the relations, Eq. (11) of Appendix A, are valid.

3.3. Effective Hamiltonian of a molecule in the presence of resonance interactions

As is known from the general vibration-rotation theory [56,57], the Hamiltonian of an arbitrary polyatomic molecule can be reduced to a set of the so-called effective Hamiltonians, or, in a more general case, to a set of effective operator matrices of the form

$$H^{vib.-rot.} = \sum_{a,b}|a\rangle\langle b|H^{a,b}. \tag{9}$$

Here $|a\rangle$ and $\langle b|$ are the basic vibrational functions; the operators $H^{a,b}$ depend on the rotational operators J_α only; and summation in Eq. (9) is performed in all degenerate and/or interacting vibrational states. When, as in our case, a molecule possesses a symmetry, Eq. (9) can be rewritten in the following form:

$$\begin{aligned} H^{vib.-rot.} &= \sum_{v_\gamma,v'_{\gamma'}}\sum_{n\Gamma}[(|v\gamma\rangle \otimes \langle v'\gamma'|)^{n\Gamma} \otimes H^{n\Gamma}_{v_\gamma,v'_{\gamma'}}]^{A_1} \\ &\equiv \sum_{v_\gamma,v'_{\gamma'}}\sum_{n\Gamma}\sum_{\Omega K}[(|v\gamma\rangle \otimes \langle v'\gamma'|)^{n\Gamma} \otimes R^{\Omega(K,n\Gamma)}]^{A_1} Y^{\Omega(K,n\Gamma)}_{v_\gamma,v'_{\gamma'}}. \end{aligned} \tag{10}$$

Here $|v\gamma\rangle$ are the above discussed symmetrized vibrational functions; the operators $R^{\Omega(K,n\Gamma)}_\sigma$ are determined in Section 3.1; and $Y^{\Omega(K,n\Gamma)}_{v_\gamma,v'_{\gamma'}}$ are spectroscopic parameters. When $v = v'$ and $\gamma = \gamma'$, the parameters $Y^{\Omega(K,n\Gamma)}_{v_\gamma,v_\gamma}$ describe the rotational structure of the vibrational state $(v\gamma)$. If $\gamma = \gamma'$, but $v \ne v'$, the parameters $Y^{\Omega(K,n\Gamma)}_{v_\gamma,v'_\gamma}$ describe the Fermi-type interactions. If $\gamma \ne \gamma'$ (v and v' are arbitrary), the parameters $Y^{\Omega(K,n\Gamma)}_{v_\gamma,v'_{\gamma'}}$ describe the Coriolis-type interactions.

The general formula, Eq. (10), is valid for an arbitrary polyatomic molecule (the forms of the operators $H^{n\Gamma}_{v_\gamma,v'_{\gamma'}}$ for different asymmetric and symmetric top molecules are presented, *e.g.*, in [58–61] and [62-69], respectively). If we use the information from Sections 3.1 and 3.2 and Appendices A–C for the spherical top XY_4 (T_d) molecule, then it can be readily shown that the parameters (operators) describing the rotational structure of the ground vibrational state and the parameters (operators) responsible for description of the ro-vibrational structure of the dyad $(0100, E)/(0001, F_2)$, have the form presented in Table 1 (in Table 1 only parameters (operators) with $\Omega \le 6$ are presented).

Knowledge of the rotational operators in the effective Hamiltonian, Eq. (10), and of the basic wave functions, Eqs. (7) and (8), permitted us to create an efficient Fortran code SPHETOM (SPHErical TOp Molecules) which allows both assigning ro-vibrational transitions and fitting spectroscopic parameters $Y^{\Omega(K,n\Gamma)}_{v_\gamma,v'_{\gamma'}}$ of the Hamiltonian, Eq. (10). In the next section we will present results of the analysis of the high resolution spectrum of $^{76}GeH_4/^{74}GeH_4$ in the spectral region of the dyad of strongly interacting bands ν_4 and ν_2 which was made with the SPHETOM code.

Some words should be said concerning the code used in the present study for the analysis of experimental data. Presently, the mostly efficient software for ro-vibrational analysis of high resolution spectra of spherical top molecules is the XTDS program package, Ref. [70], equipped with graphical user interface, Ref. [71]. Unfortunately, for users it is a "black box". Sometimes it is not too

Table 1
Parameters $Y^{\Omega(K,n\Gamma)}_{v_\gamma,v'_{\gamma'}}$ of effective Hamiltonian of the XY_4 (T_d) molecule.

$(v\gamma)$	$(v'\gamma')$	$\Omega(K,n\Gamma)$	$(v\gamma)$	$(v'\gamma')$	$\Omega(K,n\Gamma)$
$(0000,A_1)$	$(0000,A_1)$	$2(0,A_1)$	$(0001,F_2)$	$(0001,F_2)$	$4(4,E)$
$(0000,A_1)$	$(0000,A_1)$	$4(0,A_1)$	$(0001,F_2)$	$(0001,F_2)$	$4(4,F_2)$
$(0000,A_1)$	$(0000,A_1)$	$4(4,A_1)$	$(0001,F_2)$	$(0001,F_2)$	$5(1,F_1)$
$(0000,A_1)$	$(0000,A_1)$	$6(0,A_1)$	$(0001,F_2)$	$(0001,F_2)$	$5(3,F_1)$
$(0000,A_1)$	$(0000,A_1)$	$6(4,A_1)$	$(0001,F_2)$	$(0001,F_2)$	$5(5,F_1)$
$(0000,A_1)$	$(0000,A_1)$	$6(6,A_1)$	$(0001,F_2)$	$(0001,F_2)$	$5(5,F_1)$
$(0000,A_1)$	$(0000,A_1)$	$8(0,A_1)$	$(0001,F_2)$	$(0001,F_2)$	$6(0,A_1)$
$(0000,A_1)$	$(0000,A_1)$	$8(4,A_1)$	$(0001,F_2)$	$(0001,F_2)$	$6(2,E)$
$(0000,A_1)$	$(0000,A_1)$	$8(6,A_1)$	$(0001,F_2)$	$(0001,F_2)$	$6(2,F_2)$
$(0000,A_1)$	$(0000,A_1)$	$8(8,A_1)$	$(0001,F_2)$	$(0001,F_2)$	$6(4,A_1)$
$(0100,E)$	$(0100,E)$	$0(0,A_1)$	$(0001,F_2)$	$(0001,F_2)$	$6(4,E)$
$(0100,E)$	$(0100,E)$	$2(0,A_1)$	$(0001,F_2)$	$(0001,F_2)$	$6(4,F_2)$
$(0100,E)$	$(0100,E)$	$2(2,E)$	$(0001,F_2)$	$(0001,F_2)$	$6(6,A_1)$
$(0100,E)$	$(0100,E)$	$3(3,A_2)$	$(0001,F_2)$	$(0001,F_2)$	$6(6,E)$
$(0100,E)$	$(0100,E)$	$4(0,A_1)$	$(0001,F_2)$	$(0001,F_2)$	$6(6,F_2)$
$(0100,E)$	$(0100,E)$	$4(2,E)$	$(0001,F_2)$	$(0001,F_2)$	$6(6,F_2)$
$(0100,E)$	$(0100,E)$	$4(4,A_1)$	$(0100,E)$	$(0001,F_2)$	$1(1,F_1)$
$(0100,E)$	$(0100,E)$	$4(4,E)$	$(0100,E)$	$(0001,F_2)$	$2(2,F_2)$
$(0100,E)$	$(0100,E)$	$5(3,A_2)$	$(0100,E)$	$(0001,F_2)$	$3(1,F_1)$
$(0100,E)$	$(0100,E)$	$6(0,A_1)$	$(0100,E)$	$(0001,F_2)$	$3(3,F_1)$
$(0100,E)$	$(0100,E)$	$6(2,E)$	$(0100,E)$	$(0001,F_2)$	$3(3,F_2)$
$(0100,E)$	$(0100,E)$	$6(4,A_1)$	$(0100,E)$	$(0001,F_2)$	$4(2,F_2)$
$(0100,E)$	$(0100,E)$	$6(4,E)$	$(0100,E)$	$(0001,F_2)$	$4(4,F_1)$
$(0100,E)$	$(0100,E)$	$6(6,A_1)$	$(0100,E)$	$(0001,F_2)$	$4(4,F_2)$
$(0100,E)$	$(0100,E)$	$6(6,E)$	$(0100,E)$	$(0001,F_2)$	$5(1,F_1)$
$(0001,F_2)$	$(0001,F_2)$	$0(2,A_1)$	$(0100,E)$	$(0001,F_2)$	$5(3,F_1)$
$(0001,F_2)$	$(0001,F_2)$	$1(1,F_1)$	$(0100,E)$	$(0001,F_2)$	$5(3,F_2)$
$(0001,F_2)$	$(0001,F_2)$	$2(0,A_1)$	$(0100,E)$	$(0001,F_2)$	$5(5,F_1)$
$(0001,F_2)$	$(0001,F_2)$	$2(2,E)$	$(0100,E)$	$(0001,F_2)$	$5(5,F_1)$
$(0001,F_2)$	$(0001,F_2)$	$2(2,F_2)$	$(0100,E)$	$(0001,F_2)$	$5(5,F_2)$
$(0001,F_2)$	$(0001,F_2)$	$3(1,F_1)$	$(0100,E)$	$(0001,F_2)$	$6(2,F_2)$
$(0001,F_2)$	$(0001,F_2)$	$3(3,F_1)$	$(0100,E)$	$(0001,F_2)$	$6(4,F_1)$
$(0001,F_2)$	$(0001,F_2)$	$4(0,A_1)$	$(0100,E)$	$(0001,F_2)$	$6(4,F_2)$
$(0001,F_2)$	$(0001,F_2)$	$4(2,E)$	$(0100,E)$	$(0001,F_2)$	$6(6,F_1)$
$(0001,F_2)$	$(0001,F_2)$	$4(2,F_2)$	$(0100,E)$	$(0001,F_2)$	$6(6,F_2)$
$(0001,F_2)$	$(0001,F_2)$	$4(4,A_1)$	$(0100,E)$	$(0001,F_2)$	$6(6,F_2)$

convenient, especially when one would like to make some or other changes in the codes. For example, it would be reasonable to have a possibility to analyze spectra not only "polyad by polyad" as it is provided in the XTDS program package, but (as for any other type of molecules considered in high resolution spectroscopy) for separate state (or sets of states) in higher wave length regions. In that case, of course, it is good to have an opportunity for code corrections. With the XTDS program package it is not possible just because it is a "black box". As a consequence, the SPHETOM code was made which is free of such limitation.

4. Analysis of experimental data in the dyad region

GeH_4 is a spherical top molecule. As a consequence, only transitions from the ground to the F_2-symmetry vibrational states are allowed in absorption by the symmetry of the molecule. The ν_2 is the band of E-symmetry, and its ro-vibrational transitions appear in absorption only because of strong Coriolis interaction with the allowed band, ν_4. For that reason (as is seen in Fig. 1), the irregular structure of the ν_2 band contrasts with the regular structure of the ν_4 band. In Fig. 2 one can see a small part of the experimental high resolution spectrum in the region of the R-branch of the ν_4 band. The transitions assigned to the $^{76}GeH_4$ isotopologue are marked by dark circles. One can see also weaker lines belonging to the $^{74}GeH_4$ isotopologue which are located about 0.4 cm^{-1} from the corresponding lines of the $^{76}GeH_4$ isotopologue towards the blue part of the spectrum. It should be mentioned that, as can be seen from Fig. 2, the experimental spectrum contains numerous very weak lines. To answer the question "what can it be?", we made a special set of measurements with different sample pressures. As a result we saw that the intensities of the above-mentioned very weak lines had increased proportionally to the pressure. This undoubtedly indicates that the lines belong to the sample used. We believe that they cannot be lines of the other (M=73, 72, 70) isotopologues of $^{M}GeH_4$, because there are no characteristic line clusters in the spectrum. So, one can expect that they are lines corresponding to the "hot" dyad–pentad transitions of $^{76}GeH_4$ (the ratio of populations of the "dyad" vibrational states to the population of the ground vibrational state at room temperature changed from 0.019 for the (0001) state to 0.011 for the (0100) one). However, the correct answer to that question can be given only after the corresponding analysis of the spectra in the pentad region.

Assignments of the transitions were made simultaneously with the fit of parameters of the ground vibrational state and of the upper vibrational states, $(0100, E)$ and $(0001, F_2)$. As a result, we were able to assign 1922 transitions with $J^{max.} = 26$ to the $^{76}GeH_4$ isotopologue and 788 transitions with $J^{max.} = 24$ to the $^{74}GeH_4$ isotopologue. As an illustration, a small part of experimentally recorded transitions is shown in column 1 of Table 2 together with the values of absorbance (column 4) and assignment of transitions (columns 2 and 3). Columns 6 and 7 show to which band and isotopologue ($^{76}GeH_4$ or $^{74}GeH_4$) the line belongs. Values of $\Delta = \nu_{exp.} - \nu_{calc.}$ are listed in column 5. The recorded spectrum ("W" or "S") to which the transition belongs is specified in column 8. A complete list of assigned transitions is given in the Supplementary materials to the present paper.

As was noted above, the fit of the parameters of the effective Hamiltonian was made with the SPHETOM Fortran code. The weighted least square fit procedure was used. In this case, weights of isolated (unblended) not very weak and unsaturated lines have been taken as 100.

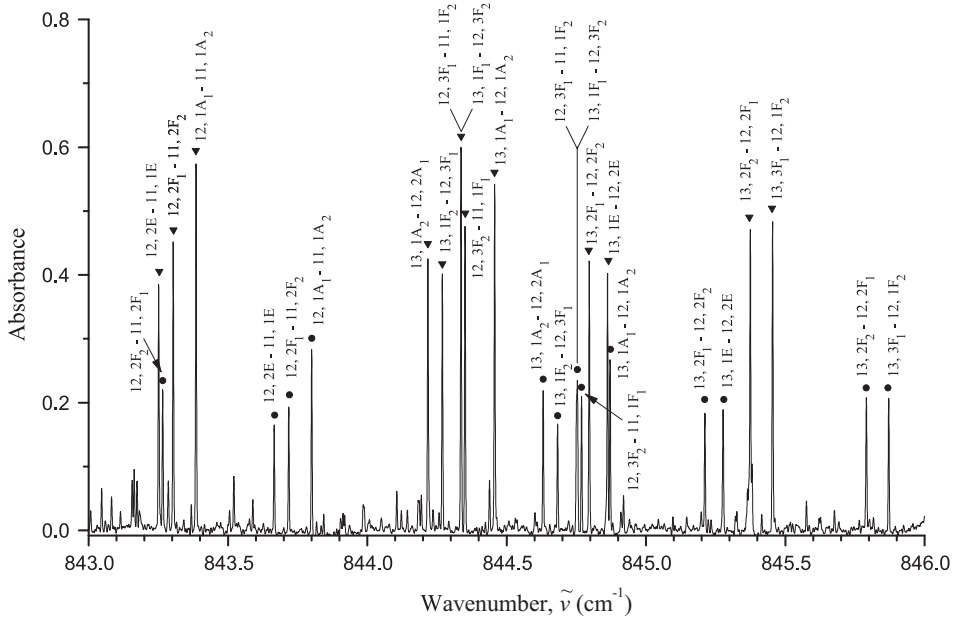

Fig. 2. Small portion of the high resolution spectrum of $^{76}GeH_4$ and $^{74}GeH_4$ in the region of the R-branch of the ν_4 band ("black" spectrum). The transitions assigned to the $^{76}GeH_4$ and $^{74}GeH_4$ isotopologues are marked by dark triangles and circles, respectively. Numerous very weak lines belong probably to the "hot" dyad–pentad bands.

Table 2
Small part of the observed transition wavenumbers of $^{M}GeH_4$ ($M = 76, 74$) in the dyad region.

Wavenumber, cm^{-1}	J	n	γ	J'	n'	γ'	Absorb.	Δ, in 10^{-4} cm^{-1}	Band	Species	Spectrum
1	2			3			4	5	6	7	8
781.42018	11	3	A_1	12	1	A_2	18.4	0.5	ν_4	74	W
781.64008	12	3	A_2	13	1	A_1	42.5	−0.3	ν_4	76	W
781.89355	12	9	F_2	13	2	F_1	31.2	−0.3	ν_4	76	W
781.96851	12	3	A_2	13	1	A_1	15.5	−0.0	ν_4	74	W
781.99308	12	6	E	13	1	E	27.1	−0.4	ν_4	76	W
782.22325	12	9	F_2	13	2	F_1	13.5	0.4	ν_4	74	W
782.32310	12	6	E	13	1	E	8.5	−1.0	ν_4	74	W
782.70904	11	8	F_1	12	2	F_2	38.9	0.0	ν_4	76	W
782.81368	13	3	A_1	14	1	A_2	35.5	0.1	ν_4	76	W
782.82592	13	10	F_1	14	1	F_2	30.4	−0.4	ν_4	76	W
782.83204	13	7	E	14	1	E	16.9	0.3	ν_4	76	W
782.96638	11	5	E	12	2	E	27.9	−0.5	ν_4	76	W
783.03556	11	8	F_1	12	2	F_2	14.0	0.2	ν_4	74	W
783.15113	13	3	A_1	14	1	A_2	14.9	−0.2	ν_4	74	W
783.16344	13	10	F_1	14	1	F_2	10.3	−0.5	ν_4	74	W
783.16947	13	7	E	14	1	E	4.0	−1.0	ν_4	74	W
783.29417	11	5	E	12	2	E	12.2	0.5	ν_4	74	W
783.32624	11	1	A_1	11	1	A_2	9.2	−1.4	ν_4	74	S
783.34058	11	3	F_1	11	2	F_2	4.4	−1.7	ν_4	74	S
783.58539	5	2	F_2	6	1	F_1	12.8	1.2	ν_4	76	S
783.87914	5	2	F_1	6	2	F_2	26.5	1.1	ν_4	76	S
784.14727	10	6	F_2	11	3	F_1	41.9	0.3	ν_4	76	W
784.36405	10	4	E	11	2	E	31.3	−0.1	ν_4	76	W
784.47003	10	6	F_2	11	3	F_1	15.4	−0.3	ν_4	74	W
784.60230	11	7	F_2	12	2	F_1	37.6	−0.0	ν_4	76	W
784.68802	10	4	E	11	2	E	14.5	−0.3	ν_4	74	W
784.80961	10	6	F_1	11	3	F_2	38.5	−0.5	ν_4	76	W
784.90444	11	9	F_1	12	1	F_2	30.8	0.1	ν_4	76	W
784.93603	11	7	F_2	12	2	F_1	13.4	−0.4	ν_4	74	W
785.07487	10	1	A_2	10	1	A_1	28.0	−0.3	ν_4	76	S
785.13570	10	6	F_1	11	3	F_2	18.3	0.4	ν_4	74	W
785.23962	11	9	F_1	12	1	F_2	15.3	−0.5	ν_4	74	W
785.32925	12	9	F_1	13	1	F_2	34.3	0.0	ν_4	76	W
785.34826	12	10	F_2	13	1	F_1	31.3	−0.4	ν_4	76	W
785.67071	12	9	F_1	13	1	F_2	13.9	−0.8	ν_4	74	W
785.68996	12	10	F_2	13	1	F_1	13.7	0.3	ν_4	74	W
786.19938	10	7	F_2	11	2	F_1	42.7	−0.2	ν_4	76	W
786.53327	10	7	F_2	11	2	F_1	18.5	0.0	ν_4	74	W
787.35952	10	5	E	11	2	E	4.6	−1.0	ν_4	76	S
787.43820	10	5	E	11	1	E	29.5	−0.1	ν_4	76	W
787.55322	10	7	F_1	11	3	F_2	5.9	0.1	ν_4	76	S
787.62504	10	7	F_1	11	2	F_2	44.5	−1.2	ν_4	76	W
787.77675	10	5	E	11	1	E	13.6	−0.5	ν_4	74	W
787.82842	11	6	E	12	1	E	29.1	−0.7	ν_4	76	W
787.84305	11	8	F_2	12	1	F_1	33.6	−0.8	ν_4	76	W
787.86207	9	5	F_1	10	3	F_2	38.0	−0.4	ν_4	76	W
787.87129	11	3	A_2	12	1	A_1	34.3	−0.1	ν_4	76	W

787.90787	10	3	A_1	11	1	A_2	37.7	0.2	ν_4	76	W
787.96466	10	7	F_1	11	2	F_2	16.7	−0.1	ν_4	74	W
788.17408	11	6	E	12	1	E	11.7	1.2	ν_4	74	W
788.18893	11	8	F_2	12	1	F_1	18.9	2.5	ν_4	74	W
788.19388	9	4	E	10	2	E	49.3	−2.0	ν_4	76	W
788.21710	11	3	A_2	12	1	A_1	24.0	1.2	ν_4	74	W
788.24869	10	3	A_1	11	1	A_2	24.4	−0.0	ν_4	74	W
788.38981	9	1	F_2	9	3	F_1	6.1	3.4	ν_4	76	S
788.49855	9	6	F_2	10	2	F_1	37.9	−1.2	ν_4	76	W
788.52742	9	4	E	10	2	E	15.0	0.9	ν_4	74	W
788.83348	9	6	F_2	10	2	F_1	19.1	0.1	ν_4	74	W
789.17373	9	2	E	9	1	E	17.4	0.0	ν_4	76	S
789.21956	9	1	A_2	9	1	A_1	22.3	−1.0	ν_4	76	S
789.49558	9	3	A_2	10	1	A_1	42.2	−0.4	ν_4	76	W
789.83609	9	3	A_2	10	1	A_1	23.7	−0.4	ν_4	74	W
790.01257	4	2	F_2	5	2	F_1	12.2	1.4	ν_4	74	S
790.25518	9	7	F_2	10	2	F_1	13.4	2.7	ν_4	76	S
790.31790	10	8	F_1	11	1	F_2	37.6	−0.1	ν_4	76	W
790.36036	10	8	F_2	11	1	F_1	35.4	−0.2	ν_4	76	W
790.61847	9	6	F_1	10	2	F_2	45.3	−0.4	ν_4	76	W
790.63706	9	7	F_2	10	1	F_1	20.8	−0.3	ν_4	74	W
790.66717	10	8	F_1	11	1	F_2	19.5	−0.6	ν_4	74	W
790.70983	10	8	F_2	11	1	F_1	19.4	−0.8	ν_4	74	W
790.96352	9	6	F_1	10	2	F_2	18.7	−1.0	ν_4	74	W
791.32539	8	2	A_1	9	1	A_2	47.9	−0.8	ν_4	76	W
791.56530	8	5	F_1	9	2	F_2	44.0	0.0	ν_4	76	W
791.66486	8	2	A_1	9	1	A_2	30.2	0.2	ν_4	74	W
791.86704	8	5	F_2	9	3	F_1	38.2	−0.3	ν_4	76	W
791.90593	8	5	F_1	9	2	F_2	19.0	−0.0	ν_4	74	W
792.20922	8	5	F_2	9	3	F_1	23.5	−0.2	ν_4	74	W
792.30902	8	2	F_1	8	1	F_2	16.9	1.4	ν_4	76	S
792.35480	8	2	F_2	8	2	F_1	15.6	−0.3	ν_4	76	S
792.50146	8	2	A_2	9	1	A_1	45.4	0.1	ν_4	76	W
792.76251	9	2	A_1	10	1	A_2	51.1	−0.1	ν_4	76	W
792.82893	9	7	F_1	10	1	F_2	37.6	−0.3	ν_4	76	W
792.84634	8	2	A_2	9	1	A_1	24.4	−0.1	ν_4	74	W
792.85897	9	5	E	10	1	E	33.0	−0.5	ν_4	76	W
793.11543	9	2	A_1	10	1	A_2	27.0	−0.1	ν_4	74	W

Table 3
Spectroscopic parameters $Y^{\Omega(K,n\Gamma)}_{v_\gamma,v'_{\gamma'}}$ of the ground vibrational state of germane (in cm^{-1})[a,b].

$\Omega(K,n\Gamma)$	$^{76}GeH_4$	$^{74}GeH_4$
1	2	3
$2(0,A_1)$	2.695870305(528)	2.695864734(234)
$4(0,A_1)10^4$	−0.3341682(330)	−0.3341682
$4(4,A_1)10^4$	−0.24753264(156)	−0.24753264
$6(0,A_1)10^8$	0.114368(658)	0.114368
$6(4,A_1)10^8$	0.1187243(333)	0.1187243
$6(6,A_1)10^8$	0.0577831(104)	0.0577831

[a] The $(v\gamma)=(v'\gamma')=(0000,A_1)$ in Table 3.
[b] Values in parentheses are 1σ statistical confidence intervals. Parameters of $^{74}GeH_4$ presented without confidence intervals were constrained to the values of corresponding parameters of the $^{76}GeH_4$ isotopologue and were fixed in the fit.

Table 4
Spectroscopic parameters $Y^{\Omega(K,n\Gamma)}_{v_\gamma,v'_{\gamma'}}$ of the $(0100,E)$ vibrational state of germane (in cm^{-1})[a,b].

$\Omega(K,n\Gamma)$	$^{76}GeH_4$	$^{74}GeH_4$
1	2	3
$0(0,A_1)$	929.9130275(120)	929.9093056(153)
$2(0,A_1)$	2.695870305	2.695870305
$2(2,E)10^2$	3.051146(154)	3.0515281(155)
$3(3,A_2)10^4$	1.80944(463)	1.80944
$4(0,A_1)10^4$	−0.3382202(928)	−0.3382202
$4(2,E)10^6$	−2.02994(673)	−2.02994
$4(4,A_1)10^5$	−2.4450064(858)	−2.4450064
$4(4,E)10^6$	−1.49638(965)	−1.49638
$6(0,A_1)10^8$	0.114368	0.114368
$6(4,A_1)10^8$	0.1187243	0.1187243
$6(6,A_1)10^8$	0.0577831	0.0577831

[a] The $(v\gamma)=(v'\gamma')=(0100,E)$ in Table 4.
[b] Values in parentheses are 1σ statistical confidence intervals. Parameters presented in column 2 without confidence intervals were constrained to their values from the ground vibrational state and were fixed in the fit. Analogously, parameters of $^{74}GeH_4$ presented in column 3 without confidence intervals were constrained to the values of corresponding parameters of the $^{76}GeH_4$ isotopologue and were fixed in the fit.

Saturated lines were not used at all. Weak lines were used in the fit with the weight 1. 36 parameters were fitted (6 parameters of the ground vibrational state and 30 parameters of the dyad): they are the 6, 7, and 13 parameters of the ground, $(0100,E)$, and $(0001,F_2)$ vibrational states, respectively, and 10 parameters which describe the Coriolis interaction between the $(0100,E)$ and $(0001,F_2)$ states. Obtained parameters are presented in column 2 of Tables 3–6 together with their 1σ statistical confidence intervals. A set of 36 parameters reproduces the initial 1922 experimental line positions of the $^{76}GeH_4$ isotopologue with the root-mean square deviation $d_{rms}=1.81\times10^{-4}$ cm^{-1} ($d_{rms}=1.76\times10^{-4}$ cm^{-1} for the ν_4 band, and $d_{rms}=1.86\times10^{-4}$ cm^{-1} for the ν_2 band), which is comparable with experimental uncertainties (see the statistical information in Table 7). Values of rotational energies of the

Table 5
Spectroscopic parameters $Y^{\Omega(K,n\Gamma)}_{v_\gamma,v'_{\gamma'}}$ of the $(0001,F_2)$ vibrational state of germane (in cm^{-1})[a,b].

$\Omega(K,n\Gamma)$	$^{76}GeH_4$	$^{74}GeH_4$
1	2	3
$0(0,A_1)$	820.3270025(104)	820.7118508(732)
$1(1,F_1)$	7.38069370(334)	7.37317292(255)
$2(0,A_1)$	2.696930760(819)	2.696932024(127)
$2(2,E)10^2$	0.42000477(979)	0.42387205(143)
$2(2,F_2)10^2$	2.469295(136)	2.2469831(125)
$3(1,F_1)10^4$	−1.881200(667)	−1.879439(789)
$3(3,F_1)10^4$	−2.21249(629)	−2.21249
$4(0,A_1)10^4$	−0.3378212(812)	−0.3378212
$4(2,F_2)10^6$	−1.8768(130)	−1.8768
$4(4,A_1)10^5$	−2.6203003(742)	−2.6203003
$5(1,F_1)10^8$	1.59831(356)	1.59831
$5(3,F_1)10^8$	1.80981(380)	1.80981
$6(0,A_1)10^8$	0.118644(873)	0.118644
$6(4,A_1)10^8$	0.1187243	0.1187243
$6(6,A_1)10^8$	0.0577831	0.0577831

[a] The $(v\gamma)=(v'\gamma')=(0001,F_2)$ in Table 5.
[b] See footnote (b) to Table 4.

Table 6
Spectroscopic parameters $Y^{\Omega(K,n\Gamma)}_{v_\gamma,v'_{\gamma'}}$ of the $(0100,E)/(0001,F_2)$ Coriolis interaction (in cm^{-1})[a,b].

$\Omega(K,n\Gamma)$	$^{76}GeH_4$	$^{74}GeH_4$
1	2	3
$1(1,F_1)$	−5.19969250(157)	−5.20319458(664)
$2(2,F_2)10^2$	−4.922900(411)	−4.919207(275)
$3(1,F_1)10^3$	−0.3144712(575)	−0.3144712
$3(3,F_2)10^4$	0.637838(440)	0.637838
$4(2,F_2)10^6$	−1.1317(156)	−1.1317
$4(4,F_1)10^6$	−1.71376(279)	−1.71376
$4(4,F_2)10^6$	−1.938780(675)	−1.938780
$5(1,F_1)10^8$	−1.41723(673)	−1.41723
$5(3,F_1)10^8$	1.45888(645)	1.45888
$5(3,F_2)10^9$	6.2773(710)	6.2773

[a] The $(v\gamma)=(0100,E)$ and $(v'\gamma')=(0001,F_2)$ in Table 6.
[b] Values in parentheses are 1σ statistical confidence intervals. Parameters of $^{74}GeH_4$ presented without confidence intervals were constrained to the values of corresponding parameters of the $^{76}GeH_4$ isotopologue and were fixed in the fit.

Table 7
Statistical information on the studied bands of germane.

Isotopomer	Band	Canter (cm^{-1})	J^{max}	$N_{tr.}$[a]	$N_{en.}$[b]	$n_{par.}$[c]	d_{rms} (10^{-4} cm^{-1})
$^{76}GeH_4$	ν_2	929.91303	23	805	318	30	1.86
$^{76}GeH_4$	ν_4	820.32700	26	1117	588		1.76
$^{76}GeH_4$	*gr.*		27			6	
$^{74}GeH_4$	ν_2	929.90931	21	245	163	10	2.52
$^{74}GeH_4$	ν_4	820.71185	24	543	457		1.79
$^{74}GeH_4$	*gr.*		25			1	

[a] The $N_{tr.}$ is the number of transitions assigned to the band.
[b] The $N_{en.}$ is the number of energy levels of the upper vibrational state.
[c] The $n_{par.}$ is the number of fitted parameters. For $^{74}GeH_4$, the unfitted parameters were fixed to the values of corresponding parameters of $^{76}GeH_4$.

Table 8
Rotational energies of the ground vibrational state of $^{76}GeH_4$ and $^{74}GeH_4$ (in cm^{-1}).

J'	n	γ	$E(M=76)$	$E(M=74)$	J'	n'	γ'	$E(M=76)$	$E(M=74)$
	1		2	3		1		2	3
0	1	A_1	0.000000	0.000000	10	2	F_1	296.183713	296.183100
1	1	F_1	5.391607	5.391596	10	1	F_2	296.077588	296.076975
2	1	E	16.173938	16.173904	10	2	F_2	296.137875	296.137262
2	1	F_2	16.174073	16.174040	10	3	F_2	296.196851	296.196238
3	1	A_2	32.346446	32.346379	11	1	A_2	355.257086	355.256350
3	1	F_1	32.345227	32.345160	11	1	E	355.269254	355.268519
3	1	F_2	32.345769	32.345702	11	2	E	355.347845	355.347110
4	1	A_1	53.902153	53.902041	11	1	F_1	355.176351	355.175615
4	1	E	53.903778	53.903667	11	2	F_1	355.305575	355.304839
4	1	F_1	53.903101	53.902990	11	3	F_1	355.352789	355.352054
4	1	F_2	53.905808	53.905697	11	1	F_2	355.177533	355.176798
5	1	E	80.848905	80.848738	11	2	F_2	355.264496	355.263761
5	1	F_1	80.842344	80.842177	11	3	F_2	355.336457	355.335721
5	2	F_1	80.849784	80.849617	12	1	A_1	419.603508	419.602639
5	1	F_2	80.844173	80.844006	12	2	A_1	419.858995	419.858126
6	1	A_1	113.176205	113.175971	12	1	A_2	419.830815	419.829946
6	1	A_2	113.163238	113.163004	12	1	E	419.604925	419.604056
6	1	E	113.159985	113.159751	12	2	E	419.782153	419.781284
6	1	F_1	113.174178	113.173944	12	1	F_1	419.604443	419.603574
6	1	F_2	113.160793	113.160559	12	2	F_1	419.726051	419.725182
6	2	F_2	113.171883	113.171649	12	3	F_1	419.852775	419.851906
7	1	A_2	150.865528	150.865216	12	1	F_2	419.717041	419.716172
7	1	E	150.873651	150.873339	12	2	F_2	419.789769	419.788900
7	1	F_1	150.849564	150.849252	12	3	F_2	419.844743	419.843874
7	2	F_1	150.878019	150.877707	13	1	A_1	489.508938	489.507924
7	1	F_2	150.851377	150.851065	13	1	A_2	489.628297	489.627283
7	2	F_2	150.870811	150.870499	13	1	E	489.496642	489.495628
8	1	A_1	193.903423	193.903022	13	2	E	489.689212	489.688198
8	1	E	193.906071	193.905669	13	1	F_1	489.348159	489.347146
8	2	E	193.949880	193.949479	13	2	F_1	489.500208	489.499194
8	1	F_1	193.905092	193.904691	13	3	F_1	489.586994	489.585980
8	2	F_1	193.941425	193.941024	13	4	F_1	489.698156	489.697142
8	1	F_2	193.931803	193.931402	13	1	F_2	489.348905	489.347892
8	2	F_2	193.952423	193.952022	13	2	F_2	489.603369	489.602355
9	1	A_1	242.374560	242.374059	13	3	F_2	489.680084	489.679070
9	1	A_2	242.396070	242.395568	14	1	A_1	564.694825	564.693655
9	1	E	242.358292	242.357791	14	1	A_2	564.397258	564.396088
9	1	F_1	242.316247	242.315745	14	1	E	564.396404	564.395234
9	2	F_1	242.361508	242.361007	14	2	E	564.728314	564.727144
9	3	F_1	242.386903	242.386401	14	3	E	564.862565	564.861395
9	1	F_2	242.317962	242.317460	14	1	F_1	564.592940	564.591770
9	2	F_2	242.392047	242.391546	14	2	F_1	564.715350	564.714180
10	1	A_1	296.164978	296.164365	14	3	F_1	564.850085	564.848915
10	1	A_2	296.079110	296.078497	14	1	F_2	564.396687	564.395517
10	1	E	296.076885	296.076272	14	2	F_2	564.586515	564.585345
10	2	E	296.189922	296.189309	14	3	F_2	564.773253	564.772083
10	1	F_1	296.145125	296.144512	14	4	F_2	564.869800	564.868630
15	1	A_1	645.335814	645.334477	18	3	E	918.421795	918.419889

Table 8 (*continued*)

J'	n	γ	$E(M=76)$	$E(M=74)$	J'	n'	γ'	$E(M=76)$	$E(M=74)$
15	1	A_2	644.970977	644.969640	18	1	F_1	917.778534	917.776629
15	2	A_2	645.366892	645.365555	18	2	F_1	918.091110	918.089205
15	1	E	644.979152	644.977815	18	3	F_1	918.344669	918.342764
15	2	E	645.223164	645.221827	18	4	F_1	918.665042	918.663137
15	1	F_1	644.735295	644.733958	18	1	F_2	917.348806	917.346900
15	2	F_1	645.125763	645.124426	18	2	F_2	917.775678	917.773772
15	3	F_1	645.237194	645.235857	18	3	F_2	918.275431	918.273526
15	4	F_1	645.349299	645.347962	18	4	F_2	918.443862	918.441957
15	1	F_2	644.735719	644.734382	18	5	F_2	918.655314	918.653409
15	2	F_2	644.976266	644.974929	19	1	A_1	1019.924199	1019.922082
15	3	F_2	645.154056	645.152719	19	1	A_2	1019.203562	1019.201445
15	4	F_2	645.359004	645.357667	19	2	A_2	1020.092454	1020.090337
16	1	A_1	730.350393	730.348877	19	1	E	1019.206860	1019.204743
16	2	A_1	731.029578	731.028063	19	2	E	1019.825133	1019.823016
16	1	A_2	730.880936	730.879421	19	3	E	1020.335156	1020.333039
16	1	E	730.350861	730.349346	19	1	F_1	1018.698866	1018.696749
16	2	E	730.840933	730.839418	19	2	F_1	1019.577535	1019.575418
16	3	E	731.158099	731.156584	19	3	F_1	1019.846580	1019.844463
16	1	F_1	730.350704	730.349189	19	4	F_1	1020.017708	1020.015591
16	2	F_1	730.648739	730.647223	19	5	F_1	1020.344419	1020.342302
16	3	F_1	730.999496	730.997980	19	1	F_2	1018.698982	1018.696865
16	4	F_1	731.147827	731.146312	19	2	F_2	1019.205746	1019.203629
16	1	F_2	730.644082	730.642566	19	3	F_2	1019.594399	1019.592282
16	2	F_2	730.851156	730.849641	19	4	F_2	1020.057197	1020.055080
16	3	F_2	730.971611	730.970096	19	5	F_2	1020.325474	1020.323357
16	4	F_2	731.167861	731.166345	20	1	A_1	1125.259813	1125.257473
17	1	A_1	821.588940	821.587235	20	2	A_1	1126.774992	1126.772653
17	1	A_2	821.967857	821.966152	20	1	A_2	1126.322145	1126.319806
17	1	E	821.583353	821.581648	20	1	E	1125.259936	1125.257596
17	2	E	822.040644	822.038939	20	2	E	1126.301046	1126.298706
17	3	E	822.264838	822.263134	20	3	E	1126.914542	1126.912202
17	1	F_1	821.227019	821.225314	20	4	E	1127.277972	1127.275633
17	2	F_1	821.585161	821.583456	20	1	F_1	1125.259895	1125.257555
17	3	F_1	821.831848	821.830143	20	2	F_1	1125.854751	1125.852412
17	4	F_1	822.091787	822.090083	20	3	F_1	1126.652702	1126.650362
17	5	F_1	822.273266	822.271561	20	4	F_1	1126.875507	1126.873167
17	1	F_2	821.227246	821.225541	20	5	F_1	1127.268030	1127.265690
17	2	F_2	821.851314	821.849609	20	1	F_2	1125.853069	1125.850729
17	3	F_2	822.015217	822.013513	20	2	F_2	1126.307597	1126.305257
17	4	F_2	822.253080	822.251375	20	3	F_2	1126.610719	1126.608379
18	1	A_1	918.074155	918.072249	20	4	F_2	1126.969200	1126.966860
18	2	A_1	918.673467	918.671561	20	5	F_2	1127.286178	1127.283838
18	1	A_2	917.348969	917.347064	21	1	A_1	1237.704836	1237.702262
18	2	A_2	918.643570	918.641665	21	2	A_1	1239.460762	1239.458188
18	1	E	917.348724	917.346819	21	1	A_2	1238.590763	1238.588189
18	2	E	918.101055	918.099150	21	2	A_2	1239.486503	1239.483929
21	1	E	1237.702945	1237.700371	23	2	F_2	1476.931645	1476.928570
21	2	E	1238.656468	1238.653894	23	3	F_2	1477.662249	1477.659174
21	3	E	1239.071932	1239.069359	23	4	F_2	1478.643528	1478.640453
21	1	F_1	1237.013333	1237.010759	23	5	F_2	1478.966013	1478.962938

21	2	F_1	1237.703572	1237.700998	23	6	F_2	1479.571893	1479.568818
21	3	F_1	1238.234221	1238.231648	24	1	A_1	1603.234252	1603.230909
21	4	F_1	1238.847660	1238.845086	24	2	A_1	1606.147713	1606.144371
21	5	F_1	1239.102409	1239.099835	24	3	A_1	1607.469790	1607.466447
21	6	F_1	1239.470210	1239.467636	24	1	A_2	1605.112387	1605.109045
21	1	F_2	1237.013391	1237.010817	24	2	A_2	1607.449546	1607.446203
21	2	F_2	1238.245103	1238.242530	24	1	E	1603.234280	1603.230938
21	3	F_2	1238.631350	1238.628776	24	2	E	1605.104132	1605.100789
21	4	F_2	1238.993626	1238.991052	24	3	E	1606.280425	1606.277082
21	5	F_2	1239.478721	1239.476148	24	4	E	1606.825805	1606.822463
22	1	A_1	1355.354332	1355.351513	24	1	F_1	1603.234271	1603.230928
22	2	A_1	1356.494341	1356.491522	24	2	F_1	1604.270615	1604.267273
22	1	A_2	1353.940270	1353.937451	24	3	F_1	1605.771944	1605.768601
22	2	A_2	1356.320179	1356.317360	24	4	F_1	1606.230101	1606.226759
22	1	E	1353.940210	1353.937391	24	5	F_1	1606.753619	1606.750277
22	2	E	1355.367466	1355.364647	24	6	F_1	1607.463398	1607.460056
22	3	E	1356.114094	1356.111275	24	1	F_2	1604.270118	1604.266776
22	4	E	1356.912872	1356.910053	24	2	F_2	1605.106839	1605.103496
22	1	F_1	1354.736448	1354.733629	24	3	F_2	1605.741723	1605.738380
22	2	F_1	1355.362945	1355.360126	24	4	F_2	1606.476665	1606.473322
22	3	F_1	1355.856395	1355.853576	24	5	F_2	1606.862701	1606.859358
22	4	F_1	1356.454866	1356.452047	24	6	F_2	1607.456667	1607.453324
22	5	F_1	1356.904790	1356.901971	25	1	A_1	1736.731639	1736.728018
22	1	F_2	1353.940230	1353.937411	25	2	A_1	1739.706024	1739.702403
22	2	F_2	1354.735518	1354.732699	25	1	A_2	1738.415565	1738.411943
22	3	F_2	1355.810365	1355.807546	25	2	A_2	1739.871268	1739.867647
22	4	F_2	1356.150734	1356.147915	25	1	E	1736.731101	1736.727480
22	5	F_2	1356.407031	1356.404212	25	2	E	1738.454045	1738.450423
22	6	F_2	1356.920714	1356.917895	25	3	E	1739.327023	1739.323402
23	1	A_1	1478.255439	1478.252364	25	4	E	1740.540057	1740.536436
23	1	A_2	1476.930964	1476.927889	25	1	F_1	1735.559822	1735.556200
23	2	A_2	1478.766065	1478.762989	25	2	F_1	1736.731280	1736.727659
23	1	E	1476.931987	1476.928912	25	3	F_1	1737.684814	1737.681193
23	2	E	1478.195633	1478.192558	25	4	F_1	1738.952857	1738.949236
23	3	E	1479.014376	1479.011301	25	5	F_1	1739.381448	1739.377827
23	4	E	1479.579647	1479.576572	25	6	F_1	1739.779934	1739.776313
23	1	F_1	1476.020680	1476.017605	25	7	F_1	1740.546116	1740.542494
23	2	F_1	1477.655170	1477.652095	25	1	F_2	1735.559835	1735.556214
23	3	F_1	1478.212954	1478.209879	25	2	F_2	1737.688991	1737.685370
23	4	F_1	1478.572429	1478.569354	25	3	F_2	1738.440384	1738.436763
23	5	F_1	1479.069197	1479.066122	25	4	F_2	1739.057576	1739.053955
23	6	F_1	1479.586622	1479.583547	25	5	F_2	1739.830043	1739.826422
23	1	F_2	1476.020708	1476.017632	25	6	F_2	1740.533886	1740.530264
26	1	A_1	1875.374429	1875.370518	27	2	A_1	2022.230675	2022.226463
26	2	A_1	1877.546368	1877.542457	27	1	A_2	2016.932865	2016.928653
26	1	A_2	1872.975628	1872.971717	27	2	A_2	2020.325579	2020.321367
26	2	A_2	1877.002574	1876.998663	27	3	A_2	2022.245447	2022.241236
26	1	E	1872.975615	1872.971704	27	1	E	2016.933141	2016.928929
26	2	E	1875.379193	1875.375282	27	2	E	2019.138566	2019.134354
26	3	E	1876.862351	1876.858441	27	3	E	2020.562508	2020.558296
26	4	E	1877.964807	1877.960897	27	4	E	2021.297403	2021.293191
26	5	E	1878.804692	1878.800781	27	1	F_1	2015.459312	2015.455100
26	1	F_1	1874.293008	1874.289097	27	2	F_1	2018.155880	2018.151668
26	2	F_1	1875.377593	1875.373682	27	3	F_1	2019.147155	2019.142944

Table 8 (*continued*)

J'	n	γ	$E(M=76)$	$E(M=74)$	J'	n'	γ'	$E(M=76)$	$E(M=74)$
26	3	F_1	1876.255926	1876.252016	27	4	F_1	2019.879075	2019.874863
26	4	F_1	1877.424620	1877.420709	27	5	F_1	2020.754215	2020.750003
26	5	F_1	1877.915012	1877.911101	27	6	F_1	2021.336292	2021.332081
26	6	F_1	1878.799028	1878.795117	27	7	F_1	2022.235743	2022.231532
26	1	F_2	1872.975619	1872.971708	27	1	F_2	2015.459318	2015.455107
26	2	F_2	1874.292750	1874.288839	27	2	F_2	2016.933049	2016.928837
26	3	F_2	1876.233741	1876.229830	27	3	F_2	2018.158285	2018.154073
26	4	F_2	1876.898914	1876.895003	27	4	F_2	2019.945637	2019.941426
26	5	F_2	1877.323508	1877.319597	27	5	F_2	2020.479597	2020.475386
26	6	F_2	1878.015887	1878.011976	27	6	F_2	2021.236676	2021.232464
26	7	F_2	1878.810045	1878.806134	27	7	F_2	2022.240664	2022.236453
27	1	A_1	2019.165347	2019.161136					

ground vibrational state for the $^{76}GeH_4$ (column 2) and $^{74}GeH_4$ (column 3) isotopologues calculated using the parameters from Table 3 are listed in Table 8.

Some words should be said concerning the procedure of the fit. In the process of assignments of transitions we were able to obtain from the analysis of experimental data more than 100 ground state combination differences (GSCD) for the $^{76}GeH_4$ species and more than 20 GSCD for the $^{74}GeH_4$ one. Any of the GSCD was determined on the basis of transitions from the different ground state rotational states to the concrete upper ro-vibrational state of the (0001) or (0100) vibrational states. Of course, unlike the asymmetric or symmetric top molecules, usually only one line among transition-partners in a concrete GSCD is a strong enough "allowed transition". The others are weak "forbidden transitions". However, all of them are well pronounced in the experimental spectra, and the corresponding ground state combination differences can be determined without doubt. The obtained number of GSCD was more than enough for correct determination of six ground state rotational parameters. When speaking about parameters of the dyad (see Table 1), as was mentioned in Ref. [72] (see also Ref. [73]), there are 19 quasi-linear relationships among the 62 upper state parameters. It means that in a general case, the number of independent parameters is 43. In the present study the number of fitted parameters of upper states was 30 for the $^{76}GeH_4$ species and only 10 for the $^{74}GeH_4$ species (that is much less than 43).

The result of the analogous fit of transitions assigned to the $^{74}GeH_4$ isotopologue is shown in column 3 of Tables 3–6. As the value of the $(M_{76}-M_{74})/M_{76}$ ratio is very small, one can expect that the differences between absolute values of spectroscopic parameters of the same type of the $^{76}GeH_4$ and $^{74}GeH_4$ isotopologues will be nonzero only for the largest parameters. For that reason, values of the majority of parameters of the $^{74}GeH_4$ isotopologue were fixed in the fit to the values of the corresponding parameters of $^{76}GeH_4$ (they are presented in Tables 3–6 without confidence intervals). The final set of 11 fitted parameters (1 parameter of the ground vibrational state and 10 parameters of the dyad) is presented in column 3 of Tables 3–6 and reproduces the initial 788 transitions ($J^{max.}=24$) of the $^{74}GeH_4$ isotopologue with $d_{rms}=2.05\times10^{-4}$ cm^{-1} ($d_{rms}=1.79\times10^{-4}$ cm^{-1} for the ν_4 band, and $d_{rms}=2.52\times10^{-4}$ cm^{-1} for the ν_2 band). It should also be mentioned that the parameters of Tables 3–6 have the same sense as the parameters used in the XTDS program package with only one exception: the $Y^{\Omega(K,A_1)}_{v_\gamma,v_\gamma}$ parameters in our case are real spectroscopic parameters of the corresponding vibrational state, but the analogous parameters in the XTDS program package are increments to the lower polyad parameters (see, *e.g.*, Ref. [44]).

To give the reader a possibility to judge the quality of the results, Fig. 3 shows the fit residuals for line positions as a function of quantum number J. Fig. 4 presents the diagram of calculated reduced energy levels for the dyad of $^{76}GeH_4$ as defined by the equation

$$E^{red.}_{Jn\gamma}/hc = E_{Jn\gamma}/hc - B_{gr}J(J+1)+D_{gr}J^2(J+1)^2-\cdots \qquad (11)$$

Fig. 5 illustrates the comparison between the experimental spectrum for the dyad (top part of Fig. 5) and the synthetic

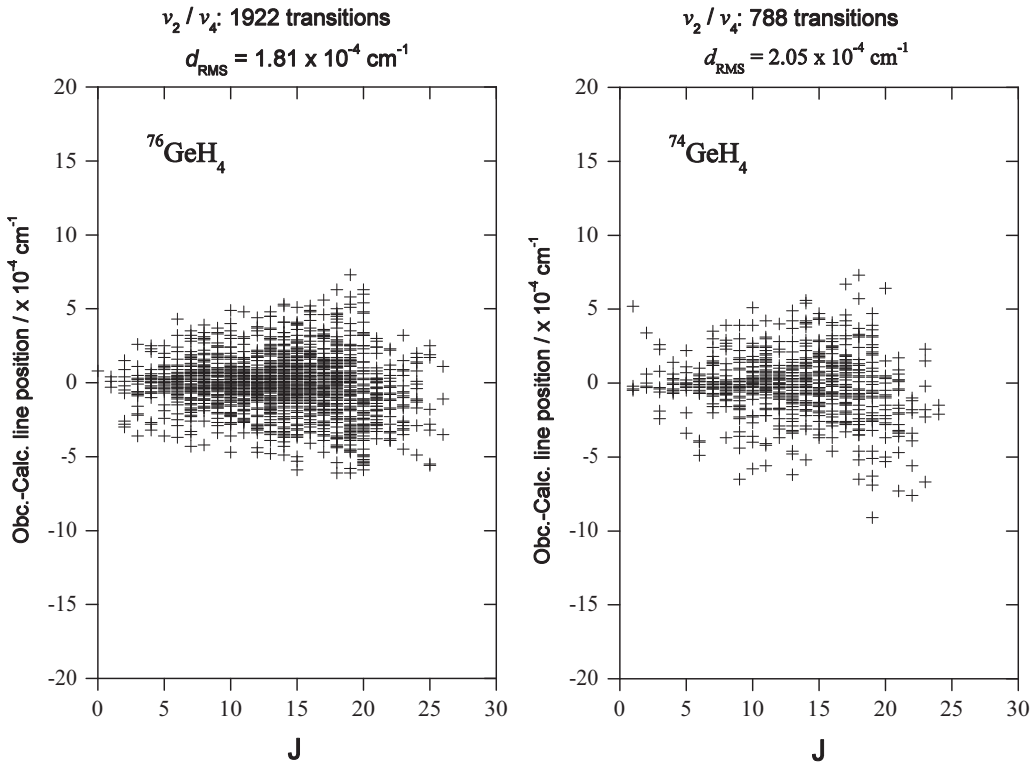

Fig. 3. Observed–calculated line positions and fit statistics for the ν_2/ν_4 dyad of the $^{76}GeH_4$ and $^{74}GeH_4$ isotopologues.

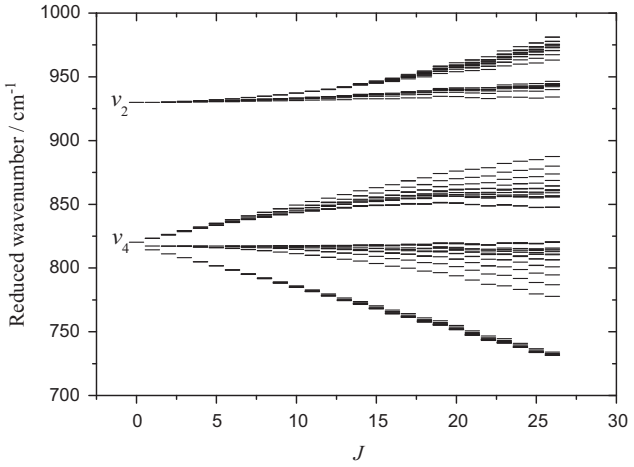

Fig. 4. Calculated reduced energy levels for the dyad of $^{76}GeH_4$ (see text for details).

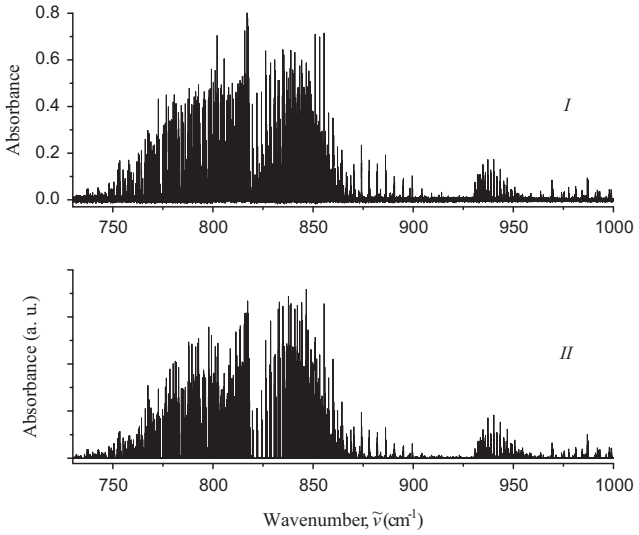

Fig. 5. Experimental (*I*) and simulated (*II*) spectra of the dyad of the $^{76}GeH_4$ and $^{74}GeH_4$ isotopologues. Experimental conditions for the spectrum I: absorption path length is 20 cm; room temperature; number of scans is 1000; sample pressure is 0.4 Torr. Simulated spectrum: line positions were calculated with the parameters obtained from the fit and presented in Tables 3–6.

spectrum (bottom part of Fig. 5) constrained on the base of the parameters derived in the present study. In all of Figs. 3–5 one can see more than satisfactory correspondence between experimental and theoretical results.

5. Conclusion

We recorded the high resolution FTIR spectrum of $^{76}GeH_4$ with a small amount of $^{74}GeH_4$ (88.1% of $^{76}GeH_4$ and 11.5% of $^{74}GeH_4$ in the sample) in the region of the dyad, ν_2/ν_4. As the result of assignment of the experimental transitions, 1922 lines with the value of $J^{max.} = 26$ and 788 lines with the value of $J^{max.} = 24$ were assigned to the $^{76}GeH_4$ and $^{74}GeH_4$ isotopologues, respectively. Analysis of the assigned transitions was made on the basis of a specially constructed Fortran code, SPHETOM. The set of 36 spectroscopic parameters reproduces the 1922 line positions of $^{76}GeH_4$ with the $d_{rms.} = 1.81 \times 10^{-4}$ cm^{-1}. Analogously, the additional set of 11 fitted parameters

reproduces the 788 line positions of $^{74}GeH_4$ with the $d_{rms.} = 2.05 \times 10^{-4}$ cm^{-1}.

Acknowledgments

This research was supported by the Foundation of the President of the Russian Federation (Grant no. MK-4872.2014.2). Part of the work was made under the project FTI-120 of the Tomsk Polytechnic University.

Appendix A. Rotational operators symmetrized in the SO(3) symmetry group

In accordance with Eqs. (1)–(5), the symmetrized rotational operators, $R_n^{\Omega(K)}$ ($0 \le \Omega \le 3$, and $0 \le K \le 3$), can be obtained in the following form:

$$\begin{aligned}
&R_0^{1(1)} = J_0 \quad J_0|Jk\rangle = k|Jk\rangle\\
&R_{+1}^{1(1)} = -J_+ = -\tfrac{1}{\sqrt{2}}\left(J_x - iJ_y\right) \quad J_+|Jk\rangle\\
&\quad = \tfrac{1}{\sqrt{2}}(J(J+1) - k(k+1))^{1/2}|Jk+1\rangle\\
&R_{-1}^{1(1)} = J_- = \tfrac{1}{\sqrt{2}}\left(J_x + iJ_y\right) \quad J_-|Jk\rangle\\
&\quad = \tfrac{1}{\sqrt{2}}(J(J+1) - k(k-1))^{1/2}|Jk-1\rangle,
\end{aligned} \tag{12}$$

$$\begin{aligned}
&R_0^{2(2)} = \sqrt{\tfrac{3}{2}}J_0^2 - \tfrac{1}{\sqrt{6}}J^2\\
&R_{\pm 1}^{2(2)} = \mp\tfrac{1}{\sqrt{2}}[J_0, J_\pm]_+\\
&R_{\pm 2}^{2(2)} = J_\pm^2\\
&R_0^{2(0)} = J^2,
\end{aligned} \tag{13}$$

$$\begin{aligned}
&R_0^{3(3)} = -\tfrac{3}{\sqrt{10}}J^2J_0 + \sqrt{\tfrac{5}{2}}J_0^3 + \tfrac{1}{\sqrt{10}}J_0\\
&R_{\pm 1}^{3(3)} = \pm\tfrac{3}{2\sqrt{15}}J_\pm J^2 \mp \tfrac{\sqrt{15}}{4}\left(J_\pm J_0^2 + J_0^2 J_\pm\right) \pm \tfrac{3}{4\sqrt{15}}J_\pm\\
&R_{\pm 2}^{3(3)} = \tfrac{\sqrt{3}}{2}\left(J_0 J_\pm^2 + J_\pm^2 J_0\right)\\
&R_{\pm 3}^{3(3)} = \mp J_\pm^3\\
&R_{\pm 1}^{3(1)} = \mp J^2 J_\pm\\
&R_0^{3(1)} = J^2 J_0,
\end{aligned} \tag{14}$$

where $J^2 = \sum_\alpha J_\alpha^2$.

Appendix B. Analytical representation of the ${}^{(K)}G^{m}_{n\Gamma\sigma}$ elements for the reduction $T_d \leftarrow SO(3)$

As was shown in Ref. [53], the elements of the G-matrix for T_d-symmetry molecule can be determined from the following analytical expressions:

$${}^{J}G^{m}_{kF_1z} = \frac{\exp(i\phi_J)[1-(-1)^J\delta_{k0}]}{2\sqrt{2}\quad(1+\delta_{k0})^{3/2}}\left[1-(-1)^{\lambda+k/2}\right]\left[\delta_{km}-(-1)^J\delta_{-km}\right], \tag{15}$$

$${}^{J}G^{m}_{kF_2y} = \frac{\exp(i\phi_J)[1-(-1)^J\delta_{k0}]}{2\sqrt{2}\quad(1+\delta_{k0})^{3/2}}\left[1-(-1)^{\lambda+k/2}\right](-i)^m\left[1-(-1)^m\right]d^J_{km}(\pi/2), \tag{16}$$

$${}^{J}G^{m}_{kF_2x} = (-1)^{\lambda+1}\frac{\exp(i\phi_J)[1-(-1)^J\delta_{k0}]}{2\sqrt{2}\quad(1+\delta_{k0})^{3/2}}\left[1-(-1)^{\lambda+k/2}\right]\left[1-(-1)^m\right]d^J_{km}(\pi/2), \tag{17}$$

$$\begin{aligned}
{}^{J}G^{m}_{kA_\lambda} = &\sum_{n=L}^{k}\alpha_{kn}^{JA_\lambda}\frac{\exp(i\chi_J)}{2\sqrt{6}}\left[1-(-1)^{\lambda+n/2}\right]\\
&\times\{[1+(-1)^m][1-(-1)^{\lambda+m/2}]d^J_{nm}(\pi/2) - (-1)^\lambda\delta_{nm}\\
&-(-1)^{\lambda+J}\delta_{-nm}\},
\end{aligned} \tag{18}$$

and

$$\begin{aligned}
{}^{J}G^{m}_{kE_\lambda} = &(-1)^{\lambda+1}\sum_{n=L}^{k}\alpha_{kn}^{JE}\frac{\exp(i\chi_J)}{4(1+2\delta_{\lambda 1})^{1/2}}\left[1+(-1)^{n/2}\right]\\
&\times\{[1+(-1)^m][1-(-1)^{\lambda+m/2}]d^J_{nm}(\pi/2) - 2\delta_{\lambda 1}[\delta_{nm}\\
&+(-1)^J\delta_{-nm}]\}.
\end{aligned} \tag{19}$$

In Eqs. (14)–(18) $\lambda = 1$ or 2, and the phases $\exp(i\phi_J)$ and $\exp(i\chi_J)$ are chosen so that $\exp(i\phi_J) = -i\exp(i\chi_J) = 1$ for odd J and $\exp(i\phi_J) = i\exp(i\chi_J) = i$ for even J (the phases are chosen in such a way that to satisfy the relations ${}^{J}G^{-m}_{k\gamma\sigma} = (-1)^m\,({}^{J}G^{-m}_{k\gamma\sigma})^*$; the validity of lasts is necessary if one wants to provide the elements of the Hamiltonian matrix to be real, see, *e.g.*, [43]). The quantities $d^J_{km}(\pi/2)$ are known from the angular momentum theory, [47]:

$$\begin{aligned}
&d^J_{km}(\pi/2) = (-1)^{k+m}\frac{1}{2^J}\left(\frac{(J+k)!(J-k)!}{(J+m)!(J-m)!}\right)^{1/2}\\
&\sum_r(-1)^r\binom{J+m}{r}\binom{J-m}{\tau+k-m}.
\end{aligned} \tag{20}$$

The index k in (14)–(18) takes the values 0, 2, 4,…, J (or $J-1$) only. In Eqs. (17) and (18) $n = L, L+4, L+8, \ldots, k$ and $L=0$ for $\Gamma = A_1$ or E, $L=2$ for $\Gamma = A_2$. The coefficients $\alpha_{kn}^{J\Gamma}$ can be obtained from simple recurrence relations:

$$\begin{aligned}
(\alpha_{kk}^{J\Gamma})^{-1/2} = &1 + \delta_{k0}(-1)^J + [4(-1)^\Gamma - 6\delta_{\Gamma E}]d^J_{kk}(\pi/2)\\
&-\sum_{l=L}^{k-4}\sum_{i\le l}\sum_{j\le l}\alpha_{li}^{J\Gamma}\alpha_{lj}^{J\Gamma}[4(-1)^\Gamma - 6\delta_{\Gamma E}]^2 d^J_{ki}(\pi/2)d^J_{kj}(\pi/2),
\end{aligned} \tag{21}$$

and

$$\alpha_{kn}^{J\Gamma} = -\alpha_{kk}^{J\Gamma}\sum_{i\ge n}^{k-4}\sum_{j\le i}\alpha_{ij}^{J\Gamma}\alpha_{in}^{J\Gamma}[4(-1)^\Gamma - 6\delta_{\Gamma E}]d^J_{kj}(\pi/2). \tag{22}$$

In Eqs. (20) and (21) the numbers k, n, i, j, and l are multiples of 4 when $\Gamma = A_1$ or E, and are even but not multiples of 4 when $\Gamma = A_2$.

Appendix C. Nonzero 3Γ-symbols of the T_d symmetry group

The nonzero 3Γ-symbols of the T_d symmetry group, which are reproduced here from Ref. [49], have the following form:

$$\begin{pmatrix} A_1 & \gamma & \gamma'\\ & s & s'\end{pmatrix} = \frac{1}{\sqrt{[\gamma]}}\delta_{\gamma\gamma'}\delta_{ss'} \quad \text{where } \gamma \text{ and } s \text{ are arbitrary;}$$

$$\begin{pmatrix} A_2 & E & E\\ & 1 & 2\end{pmatrix} = \frac{1}{\sqrt{2}}; \quad \begin{pmatrix} A_2 & F_1 & F_2\\ & \alpha & \beta\end{pmatrix} = \frac{1}{\sqrt{3}}\delta_{\alpha\beta}, \alpha, \beta = x, y, z;$$

$$\begin{pmatrix} E & E & E\\ 1 & 1 & 1\end{pmatrix} = -\begin{pmatrix} E & E & E\\ 1 & 2 & 2\end{pmatrix} = -\frac{1}{2};$$

$$\begin{pmatrix} E & F_1 & F_1\\ 1 & z & z\end{pmatrix} = \begin{pmatrix} E & F_2 & F_2\\ 1 & z & z\end{pmatrix} = -\frac{1}{\sqrt{3}};$$

$$\begin{pmatrix} E & F_1 & F_1 \\ 1 & x & x \end{pmatrix} = \begin{pmatrix} E & F_1 & F_1 \\ 1 & y & y \end{pmatrix} = \begin{pmatrix} E & F_2 & F_2 \\ 1 & x & x \end{pmatrix} = \begin{pmatrix} E & F_2 & F_2 \\ 1 & y & y \end{pmatrix} = \frac{1}{2\sqrt{3}};$$

$$\begin{pmatrix} E & F_1 & F_1 \\ 2 & x & x \end{pmatrix} = -\begin{pmatrix} E & F_1 & F_1 \\ 2 & y & y \end{pmatrix} = \begin{pmatrix} E & F_2 & F_2 \\ 2 & x & x \end{pmatrix} = -\begin{pmatrix} E & F_2 & F_2 \\ 2 & y & y \end{pmatrix} = -\frac{1}{2};$$

$$\begin{pmatrix} E & F_1 & F_2 \\ 1 & x & x \end{pmatrix} = -\begin{pmatrix} E & F_1 & F_2 \\ 1 & y & y \end{pmatrix} = -\frac{\sqrt{3}}{2}\begin{pmatrix} E & F_1 & F_2 \\ 2 & z & z \end{pmatrix} = \sqrt{3}\begin{pmatrix} E & F_1 & F_2 \\ 2 & x & x \end{pmatrix} = \sqrt{3}\begin{pmatrix} E & F_1 & F_2 \\ 2 & y & y \end{pmatrix} = -\frac{1}{2};$$

$$\begin{pmatrix} F_1 & F_1 & F_1 \\ x & y & z \end{pmatrix} = \begin{pmatrix} F_2 & F_2 & F_2 \\ x & y & z \end{pmatrix} = \begin{pmatrix} F_1 & F_1 & F_2 \\ x & y & z \end{pmatrix} = \begin{pmatrix} F_1 & F_1 & F_2 \\ y & z & x \end{pmatrix} = \begin{pmatrix} F_1 & F_1 & F_2 \\ z & x & y \end{pmatrix} = \begin{pmatrix} F_2 & F_2 & F_1 \\ x & y & z \end{pmatrix} = \begin{pmatrix} F_2 & F_2 & F_1 \\ z & x & y \end{pmatrix} = -\frac{1}{\sqrt{6}}.$$

In this case, the following relations are valid for the nonzero 3Γ-symbols:

$$\begin{pmatrix} \gamma_1 & \gamma_2 & \gamma_3 \\ s_1 & s_2 & s_3 \end{pmatrix} = \begin{pmatrix} \gamma_3 & \gamma_1 & \gamma_2 \\ s_3 & s_1 & s_2 \end{pmatrix} = \begin{pmatrix} \gamma_2 & \gamma_3 & \gamma_1 \\ s_2 & s_3 & s_1 \end{pmatrix} = (-1)^{\gamma_1+\gamma_2+\gamma_3}\begin{pmatrix} \gamma_2 & \gamma_1 & \gamma_3 \\ s_2 & s_1 & s_3 \end{pmatrix},$$

where $(-1)^{A_1} = -(-1)^{A_2} = (-1)^{E} = -(-1)^{F_1} = (-1)^{F_2} = 1$.

Appendix D. Supplementary data

Supplementary data associated with this article can be found in the online version at http://dx.doi.org/10.1016/j.jqsrt.2014.03.025.

References

[1] Haller EE. Germanium: from its discovery to SiGe devices. Mater Sci Semicond Process 2006;9:408–22.
[2] Chen F, Judge DL, Wu CYR, Caldwell J, White HP, Wagener R. High-resolution, low-temperature photoabsorption cross sections of C_2H_2, PH_3, AsH_3, and GeH_4, with application to Saturn's atmosphere. J Geophys Res 1991;96:17519–27.
[3] Atreya SK, Mahaffy PR, Niemann HB, Wong MH, Owen TC. Composition and origin of the atmosphere of Jupiter—an update, and implications for the extrasolar giant planets. Planet Space Sci 2003;51:105–12.
[4] Lodders K. Jupiter formed with more tar than ice. Astrophys J 2004;611:587–97.
[5] Lodders K. Atmospheric chemistry of the gas giant planets. Geochemical Society; Geochemical News 142 - Jan 2010. ⟨http://www.geochemsoc.org/publications/geochemicalnews/gn142jan10/atmospheric chemistryoftheg/⟩.
[6] Steward WB, Nielsen HH. The infrared absorption spectrum of germane. Phys Rev 1935;48:861–4.
[7] Lee E, Sutherland GBBM. A peculiarity in the infra-red absorption spectrum of germane. Math Proc Camb Philos Soc 1939;35:341–2.
[8] Murphy GM. Coriolis perturbations in the spectra of silane and germane. J Chem Phys 1940;8:71–8.
[9] Tindal CH, Straley JW, Nielsen HH. The infra-red spectra of SiH_4 and GeH_4. Proc Natl Acad Sci US 1941;27(4):208–12.
[10] Straley JW, Tindal CH, Nielsen HH. The vibration–rotation spectrum of GeH_4. Phys Rev 1942;62:161–5.
[11] Wilkinson GR, Wilson MK. Infrared spectra of some MH_4 molecules. J Chem Phys 1966;44:3867–74.
[12] Levin IW. Infrared intensities of the fundamental vibrations of GeH_4 and GeD_4. J Chem Phys 1965;42:1244–51.
[13] Chalmers AA, McKean DC. Infra-red intensities in GeH_4. Spectrochim Acta 1965;21:1941–5.
[14] Corice Jr. J, Fox K, Fletcher WH. Studies of absorption spectra of GeH_4 in the 2–17μ region. J Mol Spectrosc 1972;41:95–104.
[15] Kattenberg HW, Gabes W, Oskam A. Infrared and laser Raman gas spectra of GeH_4. J Mol Spectrosc 1972;44:425–42.
[16] Ozier IO, Rosenberg A. The forbidden rotational spectrum of GeH_4 in the Ground Vibronic State. Can J Phys 1973;51(17):1882–95.
[17] Curl RF, Oka T, Smith DS. The observation of a pure rotational Q-branch transition of methane by infrared-radio frequency double resonance. J Mol Spectrosc 1973;46:518–20.
[18] Curl Jr. RF. Infrared-radio frequency double resonance observations of pure rotational Q-branch transitions of methane. J Mol Spectrosc 1973;48:165–73.
[19] Kreiner WA, Oka T. Infrared-radio-frequency double resonance observations of $\Delta J = 0$ "forbidden" rotational transitions of SiH_4. Can J Phys 1975;53:2000–6.
[20] Kreiner WA, Andresen U, Oka T. Infrared-microwave double resonance spectroscopy of GeH_4. J Chem Phys 1977;66:4662–5.
[21] Kreiner WA, Orr BJ, Andresen U, Oka T. Measurement of the centrifugal-distortion dipole moment of GeH_4 using a CO_2 laser. Phys Rev A 1977;15:2298–304.
[22] Kagann RH, Ozier I, Gerry MCL. The centrifugal distortion dipole moment of silane. J Chem Phys 1976;64:3487–8.
[23] Lepage P, Brégier R, Saint-Loup R. La bande ν_3 du germane. C R Acad Sci Ser B 1976;283:179–80.
[24] Kagann RH, Ozier I, McRae GA, Gerry MCL. The distortion moment spectrum of GeH_4: the microwave Q branch. Can J Phys 1979;57:593–600.
[25] Daunt SJ, Halsey GW, Fox K, Lovell RJ, Gailar NM. High-resolution infrared spectra of ν_3 and $2\nu_3$ of germane. J Chem Phys 1978;68:1319–21.
[26] Fox K, Halsey GW, Daunt SJ, Kennedy RC. Transition moment for ν_3 of $^{74}GeH_4$. J Chem Phys 1979;70:5326–7.
[27] Kreiner WA, Magerl G, Furch B, Bonek E. IR laser sideband observations in GeH_4 and CD_4. J Chem Phys 1979;70:5016–20.
[28] Magerl G, Schupita W, Bonek E, Kreiner WA. Observation of the isotope effect in the ν_2 fundamental of germane. J Chem Phys 1980;72:395–8.
[29] Kreiner WA, Opferkuch R, Robiette AG, Turner PH. The ground-state rotational constants of germane. J Mol Spectrosc 1981;85:442–8.
[30] Lepage P, Champion JP, Robiette AG. Analysis of the ν_3 and ν_1 infrared bands of GeH_4. J Mol Spectrosc 1981;89:440–8.
[31] Cheglokov AE, Kuritsin YuA, Snegirev EP, Ulenikov ON, Vedeneeva GV. High-resolution spectroscopy of the ν_2 Q branch of GeH_4, with a computer-assisted, pulsed-diode laser spectrometer. J Mol Spectrosc 1984;105:385–96.
[32] Cheglokov AE, Kuritsin YuA, Snegirev EP, Ulenikov ON, Vedeneeva GV. Study of the ν_2 infrared band of GeH_4: Q-branch. Mol Phys 1984;53:287–94.
[33] Schaeffer RD, Lovejoy RW. Absolute line strengths of $^{74}GeH_4$ near 5 μm. J Mol Spectrosc 1985;113:310–4.
[34] Zhu Q, Thrush BA, Robiette AG. Local mode rotational structure in the (3000) Ge–H stretching overtone ($3\nu_3$) of germane. Chem Phys Lett 1988;150:181–3.
[35] Zhu Q, Thrush BA. Rotational structure near the local mode limit in the (3000) band of germane. J Chem Phys 1990;92:2691–7.
[36] Zhu Q, Qian H, Thrush BA. Rotational analysis of the (2000) and (3000) bands and vibration–rotation interaction in germane local mode states. Chem Phys Lett 1991;186:436–40.
[37] Campargue A, Vetterhöffer J, Chenevier M. Rotationally resolved overtone transitions of $^{70}GeH_4$ in the visible and near-infrared. Chem Phys Lett 1992;192:353–6.
[38] Zhu Q, Campargue A, Vetterhöffer J, Permogorov D, Stoeckel F. High resolution spectra of GeH_4 $\nu = 6$ and 7 stretch overtones. The perturbed local mode vibrational states. J Chem Phys 1993;99:2359–64.
[39] Sun F, Wang X, Liao J, Zhu Q. The (5000) local mode vibrational state of germane: a high-resolution spectroscopic study. J Mol Spectrosc 1997;184:12–21.
[40] Chen XY, Lin H, Wang XG, Deng K, Zhu QS. High-resolution Fourier transform spectrum of the (4000) local mode overtone of GeH_4: local mode effect. J Mol Struct 2000;517–518:41–51.

[41] Maki AG, Wells JS, Wavenumber calibration tables from heterodyne frequency measurements (version 1.3). Gaithersburg, MD: NIST; 1998. Available online: ⟨http://www.nist.gov/pml/data/wavenum/spectra.cfm⟩.

[42] Moret-Bailly J. Sur l'interprétation des spectres de vibration-rotation des molécules à symmétrie tétraédrique ou octaédrique. Cah Phys 1961;15:238–314.

[43] Champion JP, Pierre G, Michelot F, Moret-Bailly J. Composantes cubiques normales des tenseurs spheriques. Can J Phys 1977;55:512–20.

[44] Champion JP. Developpement complet de l'hamiltonien de vibration-rotation adapté à 1'étude des interactions dans les molécules toupies sphériques. Application aux bandes ν_2 et ν_4 de $^{12}CH_4$. Can J Phys 1977;55:1802–28.

[45] Fano U, Racah G. Irreducible tensorial sets. New York: Academic Press; 1959.

[46] Wigner EP. Quantum theory of angular momentum. New York: Academic Press; 1965.

[47] Varshalovitch DA, Moskalev AN, Khersonsky VK. Quantum theory of angular momentum. Leningrad: Nauka; 1975.

[48] Boudon V, Champion JP, Gabard T, Loëte M, Rotger M, Wenger Ch. Spherical top theory and molecular spectra. In: Quack M, Merkt F, editors. Handbook of high-resolution spectroscopy, vol. 3. Chichester: Wiley; 2011. p. 1437–60.

[49] Makushkin YuS, Ulenikov ON, Cheglokov AE. Symmetry and its applications to the problems of molecular vibration-rotation spectroscopy, Parts I and II. Tomsk: Tomsk State University Press; 1990.

[50] Ulenikov ON, Bekhtereva ES, Fomchenko AL, Litvinovskaya AG, Leroy C, Quack M. On the "expanded local mode" approach applied to the methane molecule: Isotopic substitution $CH_3D \leftarrow CH_4$ and $CHD_3 \leftarrow CH_4$. Mol Phys, 2014, in press.

[51] Moret-Bailly J, Gautier L, Montagutelli J. Clebsch–Gordan coefficients adapted to cubic symmetry. J Mol Spectrosc 1965;15:355–77.

[52] Rey M, Boudon V, Wenger Ch, Pierre G, Sartakhov B. Orientation of $O(3)$ and $SU(2) \otimes C_I$ representation in cubic point groups (O_h, T_d) for application to molecular spectroscopy. J Mol Spectrosc 2003;219:313–25.

[53] Cheglokov AE, Ulenikov ON. On determination of the analytical formulas for reduction matrices of tetrahedral-symmetry molecules. J Mol Spectrosc 1985;110:53–64.

[54] Ulenikov ON, Bekhtereva ES, Albert S, Bauerecker S, Niederer HM, Quack M. Survey of the high resolution infrared spectrum of methane ($^{12}CH_4$ and $^{13}CH_4$): partial vibrational assignment extended towards 12000 cm^{-1}. J Chem Phys, 2014, submitted for publication.

[55] Ulenikov ON, Bekhtereva ES, Albert S, Bauerecker S, Hollenstein H, Quack M. High resolution infrared spectroscopy and global vibrational analysis for the CH_3D and CHD_3 isotopomers of methane. Mol Phys 2010;108:1209–40.

[56] Nielsen HH. The vibration–rotation energies of molecules. Rev. Mod. Phys. 1951;23:90.

[57] Papousek D, Aliev MR. Molecular vibrational–rotational spectra. Amsterdam, Oxford, New York: Elsevier Scientific Publishing Company; 1982.

[58] Ulenikov ON, Sun F-G, Wang X-G, Zhu Q-S. High resolution spectroscopic study of arsine: $3\nu_3$ and $2\nu_1+\nu_3$ dyad the tendency of symmetry reduction. J Chem Phys 1996;105:7310–5.

[59] Han J-X, Ulenikov ON, Yurchinko S, Hao L-Y, Wang X-G, Zhu Q-S. High resolution photoacoustic spectrum of AsH_3 ($600A_1/E$) bands. Spectrochim Acta A 1997;53:1705–12.

[60] Hai L, Ulenikov ON, Yurchinko S, Wang X-G, Zhu Q-S. High resolution spectroscopic study of the (310) local mode combination band system of AsH_3. J Mol Spectrosc 1998;187:89–96.

[61] Ulenikov ON, Bekhtereva ES, Kozinskaia VA, Zheng J-J, He S-G, Hu S-M, et al. On the study of resonance interactions and splittings in the PH_3 molecule: ν_1, ν_3, $\nu_2+\nu_4$ and $2\nu_4$ bands. J Mol Spectrosc 2002;215:295–308.

[62] Ulenikov ON, Malikova AB, Li H-F, Qian H-B, Zhu Q-S, Thrush BA. High-resolution spectroscopic study of $2\nu_1$, $2\nu_3$, and $\nu_1+\nu_2$ stretching states: the local mode effects of H_2Se. J Chem Soc Faraday Trans 1995;91:13–6.

[63] Zhou Z-Y, Wang X-H, Zhou Z-P, Ulenikov ON, Onopenko GA, Zhu Q-S. High resolution spectroscopic study of H_2Se (40^+, 0) A_1 and (40^-, 0) B_2 stretching states: normal mode and local mode analysis. Mol Phys 1997;92:1073–81.

[64] Wang X-H, Ulenikov ON, Onopenko GA, Bekhtereva ES, He S-G, Hu S-M, et al. High resolution study of the first hexad of D_2O. J Mol Spectrosc 2000;200:25–33.

[65] Hu S-M, Ulenikov ON, Onopenko GA, Bekhtereva ES, He S-G, Wang X-H, et al. High-resolution study of strongly interacting vibrational bands of HDO in the region 7600–8100 cm^{-1}. J Mol Spectrosc 2000;203:228–34.

[66] Ulenikov ON, Bekhtereva ES, Onopenko GA, Sinitsin EA, Bürger H, Jerzembeck W. Isotopic effects in XH_3 molecules: the lowest vibrational bands of PH_2D reinvestigated. J Mol Spectrosc 2001;208:236–48.

[67] Ulenikov ON, Hu S-M, Bekhtereva ES, Onopenko GA, He S-G, Wang X-H, et al. High-resolution Fourier transform spectrum of D_2O in the region near 0.97 μm. J Mol Spectrosc 2001;210:18–27.

[68] Ulenikov ON, Gromova OV, Bekhtereva ES, Bolotova IB, Konov IA, Horneman VM, et al. High resolution analysis of the SO_2 spectrum in the 2600–2900 cm^{-1} region: $2\nu_3$, $\nu_2+2\nu_3-\nu_2$ and $2\nu_3+\nu_2$ bands. J Quant Spectrosc Radiat Transf 2012;113:500–17.

[69] Ulenikov ON, Gromova OV, Aslapovskaya YuS, Horneman VM. High resolution spectroscopic study of C_2H_4: re-analysis of the ground state and ν_4, ν_7, ν_{10}, and ν_{12} vibrational bands. J Quant Spectrosc Radiat Transf 2013;118:14–25.

[70] Wenger C, Boudon V, Champion JP, Pierre G. Highly-spherical top data system (HTDS) software for spectrum simulation of octahedral XY_6 molecules. J Quant Spectrosc Radiat Transf 2000;66:1–16.

[71] Wenger C, Boudon V, Rotger M, Sanzharov M, Champion JP. XTDS and SPVIEW: graphical tools for the analysis and simulation of high-resolution molecular spectra. J Mol Spectrosc 2008;251:102–13.

[72] Champion JP, Hilico JC, Wenger C, Brown LR. Analysis of the ν_2/ν_4 dyad of $^{12}CH_4$ and $^{13}CH_4$. J Mol Spectrosc 1989;133:256–72.

[73] Ulenikov ON. On the determination of the reduced rotational operator for polyatomic molecules. J Mol Spectrosc 1986;119:144–52.